REPORT DOCUMENTATION PAGE

Form Approved
OMB No. 0704-0188

1. REPORT DATE (DD-MM-YYYY)	2. REPORT TYPE	3. DATES COVERED (From - To)
20-12-2002	Technical Paper	

4. TITLE AND SUBTITLE

Pulse Combustion Rockets for Space Propulsion Applications

5a. CONTRACT NUMBER

5b. GRANT NUMBER

5c. PROGRAM ELEMENT NUMBER

6. AUTHOR(S)

Edward B. Coy

5d. PROJECT NUMBER
2308

5e. TASK NUMBER
M13C

5f. WORK UNIT NUMBER

7. PERFORMING ORGANIZATION NAME(S) AND ADDRESS(ES)

Air Force Research Laboratory (AFMC)
AFRL/PRSA
10 E. Saturn Blvd.
Edwards AFB, CA 93524-7680

8. PERFORMING ORGANIZATION REPORT NUMBER

AFRL-PR-ED-TP-2002-321

9. SPONSORING / MONITORING AGENCY NAME(S) AND ADDRESS(ES)

Air Force Research Laboratory (AFMC)
AFRL/PRS
5 Pollux Drive
Edwards AFB CA 93524-7048

10. SPONSOR/MONITOR'S ACRONYM(S)

11. SPONSOR/MONITOR'S NUMBER(S)
AFRL-PR-ED-TP-2002-321

12. DISTRIBUTION / AVAILABILITY STATEMENT

Approved for public release; distribution unlimited.

13. SUPPLEMENTARY NOTES

14. ABSTRACT

15. SUBJECT TERMS

16. SECURITY CLASSIFICATION OF:			17. LIMITATION OF ABSTRACT	18. NUMBER OF PAGES	19a. NAME OF RESPONSIBLE PERSON
					Leilani Richardson
a. REPORT	b. ABSTRACT	c. THIS PAGE	A		19b. TELEPHONE NUMBER (include area code)
Unclassified	Unclassified	Unclassified			(661) 275-5015

2308 M13C

Ed Coy

MEMORANDUM FOR PRS (In-House Publication)

FROM: PROI (STINFO) 27 Dec 2002

SUBJECT: Authorization for Release of Technical Information, Control Number: **AFRL-PR-ED-TP-2002-321**
Edward Coy (PRSA), "Pulse Combustion Rockets for Space Propulsion Applications"

TAL 6-1

AIAA Aerospace Sciences Conference **(Statement A)**
(Reno, NV, 6-9 January 2003) (Deadline: 06 Jan 2003)

Pulse Combustion Rockets for Space Propulsion Applications[‡]

Edward B. Coy[*]
Air Force Research Laboratory, Edwards AFB, CA 93524-7660

Abstract

Pulse combustion propulsion devices are currently being considered as alternatives to conventional constant-pressure engines. Potential advantages include reduction or elimination of pumps and/or compressors, and improved Isp for a given feed system supply pressure. In this paper a model is presented for a monopropellant-fueled, constant-volume, pulse combustor which includes finite-rate processes. A zero-dimensional model is used for the combustion chamber and a one-dimensional, quasi-steady approximation is used for the nozzle flow. The liquid spray is assumed to have a log-normal distribution of spherical droplets and the reaction rate is based on a strand burner correlation. This model was developed as a tool for designing an experimental rocket. In this paper it is used to explore the time and dimensional scales of the problem and to predict the performance and optimal geometry. The pulsed propulsion device is found to have nearly identical specific impulse as the steady-state engine operating with the same mass flow and throat area, furthermore, the nozzle optimizes at the same area ratio. Pulsed combustor behavior is found to depend on two time scales: the ratio of the heat release time to the chamber blow-down time, and the ratio of the blow-down time to the injector pulsing period. Finally, the model is used to assess potential benefits of pulsed engines for satellite applications. We briefly consider the application of pulse combustion devices in pressure-fed satellite propulsion systems and examine the effect on satellite mission.

Introduction

In a previous paper we explored the constant-volume limit of pulsed propulsion, where the combustion chamber was approximated as being time varying but spatially uniform, and the nozzle flow was approximated as one-dimensional but quasi-steady[1]. The heat release process was assumed to completely consume the propellant and to occur without change in mass in the combustion chamber, either because the injection and reaction rates are much faster than the rate of mass flow out of the nozzle, or because a hot-gas valve is located in the exit stream. In this paper we extend the analysis by considering finite-rate processes such as heat release, injection, and blowdown, and inefficiencies associated with incomplete combustion.

The type of pulse combustor considered here operates on the following cycle. Reactants are injected in a short burst during the low-pressure portion of the cycle. The spray ignites when exposed to hot residual products of the previous cycle and the chamber pressure rises as the decomposition products are produced. The chamber pressure reaches a peak as the liquid is completely consumed and then falls as the gas exits through a Delaval nozzle, generating thrust.

This engine cycle may have advantages relative to the pulsed detonation engine cycle[2] in that it may be possible to eliminate the ignition system for all but the initial starting transient. It may also be possible to eliminate the purge gas separating products and reactants. Finally, it may be possible to fill the chamber to high initial densities without generating pressures and shock waves characteristic of high-explosives (10^9 Pa).

To achieve pulsed operation the injection time must be less than the heat release time which in turn must be less than the blowdown time. Furthermore, to produce large pressure oscillations, the blowdown time must not be long relative to the injector pulsing time. If this order is not maintained then the advantages of low-pressure injection cannot be realized.

Two methods of injection may be considered: fixed frequency and fixed pressure. In general fixed frequency is preferred because it enables precise control of the mass flow rate. Fixed pressure has the advantage that it allows propellant to be injected at the point in the cycle which is optimal for achieving the desired heat

[*] Research Scientist, Aerophysics Branch

release time. Both methods result in stable operation, therefore from an analytical perspective, there is no difference. In this paper, fixed frequency operation is assumed.

Propulsion devices operating on the constant-volume, or "explosion-cycle" have been proposed in the past. Ref. 3 discusses an early attempt at building an air-breathing device. This device was fueled by a gasoline spray. The heat release time was measured to be 6-9 msec which produced a pressure rise of approximately a factor of two. It was predicted that a pressure rise time of 3 msec was needed to generate pressure ratios for viable operation.

Detonation wave engines can complete reactions on the order of 1 msec or less and generate pressure ratios on the order of 10 for air-breathing engines. For rocket engines operating on condensed phase propellants, the pressure ratios could potentially reach extremely high values. In fact, the peak pressures must be constrained by limiting the density of the initial charge to avoid spallation and extremely heavy combustion chambers. Since the pressure ratios must be limited, it is worthwhile considering alternative means for achieving combustion-generated pressure ratios. In this paper we use a correlation developed for the monopropellant nitromethane to show that very large pressure ratios can be generated from the decomposition of a spray.

Model

The model consists of standard equations for conservation of mass and energy in a control volume. A "lumped-parameter" formulation is used. The uniform chamber approximation can be made for the devices considered in this study because the transit time for a pressure wave to traverse the combustion chamber is much less than the time scale of pressure changes in the chamber. A typical value for speed of sound is 1200 m/s and a typical chamber length is 5 cm, giving a transit time of 4×10^{-5} seconds, whereas the time scale for pressure changes due to combustion and blowdown are on the order of 10^{-3} seconds.

The control volume contains the gas in the combustion chamber up to nozzle throat but not the droplets. For the continuous processes of droplet burning and chamber blowdown,

$$\dot{m}_g = \dot{m}_s - \dot{m}_e , \qquad (1)$$

$$m_g C_V \frac{dT_g}{dt} = \dot{m}_s\left(h_s + \frac{u_s^2}{2}\right) - \dot{m}_e\left(h_e + \frac{u_e^2}{2}\right) + \dot{Q}_{CV} - \dot{W}_{CV} \qquad (2)$$

where the subscript g denotes gas, s denotes spray and e denotes exit. The velocity of flow from the droplets is assumed to be negligible. The energy entering the control volume from the spray can expressed in terms of an adiabatic flame temperature, $h_S = C_P T_{AFT}$. The exiting energy can be expressed in terms of the chamber stagnation enthalpy, $C_P T_g = h_e + u_e^2/2$. The work term accounts for expansion of the control volume as droplets in the chamber are consumed, $\dot{W}_{CV} = P_g \dot{m}_S / \rho_S$. Heat transfer is neglected.

Assuming isentropic flow of a perfect gas, the exiting mass flow is calculated from the choked flow expression,

$$\dot{m}_{exit} = \frac{P_0 A^*}{\sqrt{R T_0}} \sqrt{\gamma}\left(\frac{2}{1+\gamma}\right)^{\frac{1+\gamma}{2(\gamma-1)}} \qquad (3)$$

where T_0 is the instantaneous stagnation temperature in the combustion chamber. The exiting flow is assumed to be choked at all times.

Mass flow from the droplets is obtained using the following model. The initial droplet size distribution for each injection is assumed to be adequately described by the log-normal distribution,

$$n(D_0) = \frac{N}{\sqrt{2\pi}\,\ln^2\sigma_g\; D_0} \; x \exp\left[-\frac{(\ln D_0 - \ln \overline{D}_g)^2}{2\ln^2\sigma_g}\right] \qquad (4)$$

where N is the total number of droplets, $\overline{D}_g$ is the median diameter and σ_g is the geometric standard deviation. As the droplets are consumed the distribution will change. In general, burning rate is dependent on diameter as in the case of the "D-squared Law" and the distribution transforms as, $n(D)dD = n(D_0)dD_0$, where D is the current size of the droplet which was initially D_0 at the time of injection. Thus to obtain $n(D)$ from $n(D_0)$ one must have dD_0/dD. For the case of monopropellant burning the surface regression rate is the same for all diameters so the derivative is equal to 1 and the new distribution is simply,

$$n(D,D') = \frac{N}{\sqrt{2\pi}\,\ln^2\sigma_g\,(D+D')} \quad (5)$$
$$x\exp\left[-\frac{(\ln(D+D')-\ln\overline{D}_g)^2}{2\ln^2\sigma_g}\right]$$

where D' is the amount of surface regression which has occurred since the time of injection. The total volume of liquid remaining is,

$$V(D') = \int_0^\infty \frac{\pi D^3}{6} n(D,D')\,dD \quad (6)$$

This integral has the following solution,

$$V(D') = \frac{N\pi}{6}\left[F_3(D') - 3D'F_2(D') + 3D'^2F_1(D') - D'^3F_0(D')\right] \quad (7)$$

where,

$$F_n(D') = \frac{1}{2}\exp\left(n\ln\overline{D}_g + \frac{n^2}{2}\ln^2\sigma_g\right) \quad (8)$$
$$x\left[1-erf\left(\frac{\ln D' - (\ln\overline{D}_g + n\ln^2\sigma_g)}{\sqrt{2}\ln\sigma_g}\right)\right]$$

The mass flow rate from liquid to gas used in eqns. (1) and (2) is obtained as follows,

$$\dot{m}_S = \rho_{LIQUID}\frac{dV}{dD'}\frac{dD'}{dt}. \quad (9)$$

The first derivative on the RHS is obtained from eqn. (7). The second is obtained from an empirical correlation contained in ref(4).

$$\frac{dD'}{dt}[m/s] = -.632\times10^{-9}\,P^{1.02}\,[Pa]. \quad (10)$$

Equation (7) is solved numerically along with the conservation equations for mass and energy in the control volume. To determine the liquid volume and its rate of change from any given injection, the current value of D' is subtracted from the value at time of injection.

It is worth noting that the most common method for modeling droplet burning is to discretize the distribution into several size classes and represent each class by an ODE. If the device is a pulsating combustor then each new injection adds several more ODEs. Eventually computing speed must suffer. The model presented here requires only one ODE for any number of injections. Furthermore, the results are an exact solution of the assumed log-normal distribution.

Combustion inefficiency occurs when the residence time of the propellant is insufficient for complete combustion to occur. Within the framework of the 0-D or lumped-parameter model for the combustion chamber, the residence time of the droplets is assumed to equal the residence time of the gas. Therefore, for each injection we can write the following expression for the rate of change of the number of droplets remaining in the chamber,

$$\frac{\dot{n}}{n} = \frac{\dot{m}_e}{m_g}. \quad (11)$$

The same approach used in calculating the extent of vaporization can be used here to eliminate the need to solve an equation for each injection. The formal solution for eq. (11) is,

$$n = n_0\exp\left(\int_0^t \frac{\dot{m}_e}{m_g}dt - \int_0^{t_{inj}}\frac{\dot{m}_e}{m_g}dt\right). \quad (12)$$

The first integral in (12) is solved numerically along with the conservation equations. The value at the time of injection is stored as the second integral. When the number of droplets remaining in the chamber is less than 0.01% of the number injected, the injection is eliminated.

The injection process occurs as discrete events. A finite duration injection must be simulated by breaking the continuous event into several discrete pulses spaced over the interval. Since the injection occurs instantaneously, mass flows do not occur and the mass of the gas is unchanged. Therefore, $\Delta E_{CV} = -\Delta W_{CV}$. Assuming isentropic compression the work performed on the gas can be calculated as,

$$\Delta W_{CV} = \int_{V_1}^{V_2} P\,dV = \frac{P_1V_1^\gamma}{1-\gamma}\left(V_2^{1-\gamma} - V_1^{1-\gamma}\right), \quad (13)$$

where $V_2 = V_1 - V_S$. The step change in gas temperature from the compression that occurs during an injection is, $\Delta T_g = \Delta W_{CV}/m_gC_V$.

The exiting flow is assumed to be choked at all times. If the nozzle exit pressure falls below the level at which a shock can enter the nozzle a flag is set. The data presented in this paper is for cases where a shock did not enter the nozzle.

A monopropellant simulant with the following properties was used for all the cases presented.

Gas Molecular Weight	20 gm/mol
Specific Heat Ratio	1.2
Density of Liquid	1000 Kg/m^3
Adiabatic Flame Temperature	2500 K

The instantaneous thrust is calculated using the ideal thrust equation,

$$T = PA^* \sqrt{\frac{2\gamma^2}{\gamma-1}\left(\frac{2}{\gamma+1}\right)^{(\gamma+1)/(\gamma-1)}\left[1-\left(\frac{p_e}{p}\right)^{(\gamma-1)/\gamma}\right]} + (p_e - p_a)A_e \quad (14)$$

The minimum exit pressure at which a shock will enter the nozzle is obtained from the expression,

$$\frac{p_e}{p} = \left(\frac{2\gamma}{\gamma+1}M_e^2 - \frac{\gamma-1}{\gamma+1}\right) \Big/ \left(1+\frac{\gamma-1}{2}M_e^2\right)^{\gamma/(\gamma-1)} \quad (15)$$

The exit Mach number is a function of the area ratio.

The performance parameter of interest is the specific impulse or Isp. For a steady thruster, Isp is defined as,

$$Isp = \frac{T}{g_c \dot{m}}, \quad (16)$$

where g_c is the gravitational constant. For an unsteady device Isp is,

$$Isp = \frac{\int T(t)\,dt}{g_c \int \dot{m}(t)\,dt}, \quad (17)$$

where the integration is over the duration of operation, or over a single pulse if the device has reached limit-cycle conditions, or over a sample of pulses if there is significant pulse-to-pulse variability. The mass flow rate as defined here includes the amount of propellant that is required to pump fuel into the chamber. For simplicity, we will assume a pressure fed system so that this mass need not be explicitly accounted for.

In addition to the performance, we are also interested in the magnitude of pressure oscillations,

$$P^* = \left(P_{C,MAX} - P_{C,MIN}\right)/P_{SS}, \quad (18)$$

where P_{SS} is the steady state, or high frequency limit of the chamber pressure for a given throat area and mass flow rate.

Performance

In this section some example calculations are presented which show the effects of pulsed operation on performance. Cases 1-4 in Table 1 show the effect of injection frequency for fixed geometry and average mass flow rate. Case 1 shows that injecting at 5000 Hz results in nearly constant chamber pressure (P^*=0) and represents a baseline for comparison. Cases 2-4 show that as frequency is decreased from 5000 Hz to 100 Hz, the Isp decreases slightly from 233.30s to 232.85, or 0.2%, while the minimum chamber pressure decreases from 2.51 MPa to 0.28 MPa. Thus under the conditions shown here it is possible to achieve nearly the same performance as a conventional rocket with an injection system that discharges at one tenth the pressure.

Chamber pressures for Cases 2-4 are plotted in Figure 1. Three complete cycles are shown. There is a trend towards larger chamber pressure oscillations at longer pulse periods. Decreasing the frequency at fixed engine geometry and mass flow, decreases the pressure at the time of injection.

In cases 5 and 6 the area ratio is varied above and below the baseline case to determine if the optimum value differs from that of the equivalent steady state engine. A baseline area ratio of 4.26 was used in Case 4 which is the optimized value for a steady rocket operating with the same average mass flow and throat area. In both cases, Isp decreases as Ae/A* moves away from 4.26 indicating that the optimum value is approximately the same as that of the steady engine.

In cases 7 and 8 the performance in vacuum is compared. An area ratio of 100 was arbitrarily selected. Once again the performance penalty of pulsating operation is approximately 0.2%

An alternative basis for comparing the performance of steady and pulsed systems is constant injection pressure. Again using Case 4 as the baseline, in Case 20 the nozzle throat area was decreased while average mass flow rate and injection frequency were held constant. Chamber volume was also decreased to maintain approximately the same value of P^*. The nozzle area ratio was optimized for the new value of P_{SS}. The I_{SP} of Case 20 is 273 s, an increase of 17% relative to the baseline Case 4. The increased performance is due to the higher value of P_{SS}, 15.3 MPa for Case 20 versus 2.51 MPa for Case 4. Case 20 assumes an ambient pressure of 1 bar. Figure 2 shows additional comparisons for a range of ambient pressures from 1 bar to vacuum. Nozzle area ratios were optimized based on matching exit pressure to

	1	2	3	4	5	6	7	8	20
Vol. (10^{-6} m^3)	5.50	5.50	5.50	5.50	5.50	5.50	5.50	5.50	0.902
A^* (10^{-6} m^2)	2.20	2.20	2.20	2.20	2.20	2.20	2.20	2.20	0.361
Pamb (MPa)	0.10	0.10	0.10	0.10	0.10	0.10	0.00	0.00	0.10
A_e/A^*	4.26	4.26	4.26	4.26	4.00	4.50	100	100	153
f_{ini} (Hz)	5000	500	200	100	100	100	5000	100	100
N_{cycles}	200	200	200	100	100	100	5000	100	100
m_{inj} (10^{-6} Kg)	0.70	7.0	17.5	35.0	35.0	35.0	35.0	35.0	35.0
$\overline{D}_g$ (10^{-6} m)	1.0	1.0	0.1	0.1	0.1	0.1	0.1	0.1	0.1
σ_g	1.01	1.01	1.01	1.01	1.01	1.01	1.01	1.01	1.01
I_{sp} (s)	233.30	233.29	233.16	232.64	232.58	232.60	314.40	313.85	272.78
Pc,max (MPa)	2.51	3.10	4.12	8.43	8.43	8.43	2.56	8.43	50.72
Pc,min (MPa)	2.51	1.90	1.06	0.28	0.28	0.28	2.45	0.28	2.52
P	0.00	0.48	1.22	3.24	3.24	3.24	0.05	3.24	3.15
m_{liq} (10^{-3} Kg/s)	3.5	3.5	3.5	3.5	3.5	3.5	3.5	3.5	3.5
t_{INJ} (10^{-3} s)	0.0	0.0	0.0	0.0	0.0	0.0	0.0	0.0	0.0
t_{HR} (10^{-3} s)	0.5	0.40	0.10	0.10	0.10	0.10	0.10	0.10	0.05
t_{BD} (10^{-3} s)	2.7	2.7	2.7	2.7	2.7	2.7	2.7	2.7	2.7
t_{PULSE} (10^{-3} s)	0.2	2	5	10	10	10	10	10	10
$\overline{D}_2$ (10^{-6} m)	0.1	0.1	0.1	0.1	0.1	0.1	0.1	0.1	0.1

Table 2 Pulse combustor performance calculations

ambient assuming a chamber pressure of P_{SS}. If the required area ratio exceeded 100 then 100 was used. Clearly the benefit to performance of increased P_{SS} diminishes as ambient pressure is reduced. This is simply a consequence of the diminishing effect of increasing pressure ratio.

The above discussion shows that pulsed propulsion has essentially the same performance as steady for equal values of P_{SS}. Furthermore, nozzle area ratios optimize at the same value. The potential advantage of pulsed propulsion lies in the possibility of reducing feed system pressure for a given value of P_{SS}. This may result in feed system components which are lighter, less expensive and more robust.

Pulsed Propulsion Scaling

In this section some example calculations are given to illustrate scaling principles.

If it is assumed that P_{SS} is fixed and that the heat release time is very short, then the injection period and chamber volume are the only independent variables. In figure 1 the effect of increasing the injection period at fixed volume was shown. It is also possible to show that reducing the chamber volume at fixed injection period has an identical effect. In figure 3 the volume and injection period are changed together. The baseline Case 4 is plotted with Case 9, in which pulse period and chamber volume are doubled, and Case 10, in which they are halved. In each case the chamber pressure oscillates between the same limits. The injection pressure and performance in each case are the same, but the cases with short injection periods have smaller chamber volumes.

Changing the chamber volume affects the characteristic blow down time, t_{BD}. An estimate for t_{BD} time can be defined as $t_{BD} = m_C / \dot{m}_{exit} = V / A^* \sqrt{R T_C}\, f(\gamma)$. If we consider the $\sqrt{T_C}$ dependence as a weak function of the chamber pressure then for the gas considered here $t_{BD} \approx 1.5x10^{-3} V / A^*$. Since t_{BD} is a linear function of the chamber volume, then the effect of halving or doubling volume in Cases 9 and 10 was to halve or double t_{BD}. For the conditions given for figure 3, we can conclude that chamber pressure is a function of t_{BD} / t_{PULSE} only.

This result can be extended to include any value of P_{SS} if the chamber pressure is scaled by P_{SS}. In Case 11 the throat area and the injection period are halved while in Case 12 both

	4(rep.)	9	10	11	12	13	14
Vol. (10^{-6} m^3)	5.50	11.0	2.75	5.50	5.50	5.50	5.50
A^* (10^{-6} m^2)	2.20	2.20	2.20	4.40	1.10	2.20	2.20
Pamb (MPa)	0.10	0.10	0.10	0.10	0.10	0.10	0.10
Ae/A^*	4.26	4.26	4.26	2.63	7.08	4.26	7.07
f_{inj} (Hz)	100	50	200	200	50	100	100
N_{cycles}	100	50	100	100	50	50	50
M_{inj} (10^{-6} Kg)	35.0	70.0	17.5	17.5	70.0	35.0	70.0
$\overline{D}_g$ (10^{-6} m)	1.0	1.0	1.0	1.0	1.0	10.0	10.0
σ_g	1.01	1.01	1.01	1.01	1.01	1.01	2.00
I_{sp} (s)	232.47	233.02	232.60	211.81	250.73	232.99	250.45
P_{SS} (MPa)	2.51	2.51	2.51	1.26	5.03	2.51	5.03
$P_{C,max}$ (MPa)	7.95	8.19	8.31	4.02	16.62	5.10	7.29
$P_{C,min}$ (MPa)	0.43	0.42	0.42	0.21	0.85	0.67	2.31
(Pc,max-Pc,min)/Pss	2.99	3.09	3.10	3.03	3.13	1.76	0.99
m_{liq} (10^3 Kg/s)	3.5	3.5	3.5	3.5	3.5	3.5	7.0
t_{INJ} (10^{-3} s)	0.00	0.00	0.00	0.00	0.00	0.00	0.00
t_{HR} (10^{-3} s)	0.02	0.02	0.02	0.05	0.05	2.08	14.78
t_{BD} (10^{-3} s)	3.75	7.50	1.88	1.88	7.50	3.75	3.75
t_{PULSE} (10^{-3} s)	10.00	20.00	5.00	5.00	20.00	10.00	10.00
$\overline{D}_2$ (10^{-6} m)	1.0	1.0	1.0	1.0	1.0	10.0	16.2

Table 3 Pulse combustor performance - continued

are doubled, leaving t_{BD}/t_{PULSE} unchanged. The average mass flows are the same in each case so the changes in throat area result in different values for P_{SS}. If time is also scaled by t_{PULSE} then Figure 4 shows that the non-dimensionalized chamber pressures traces are identical. The slight scatter observable in the traces is a result of a small but finite heat release times. Figure 5 extends the results of figure 4 to show the effect of varying t_{BD}/t_{PULSE}. Decreasing t_{BD}/t_{PULSE} results in larger relative changes in chamber pressure.

Figure 6 shows the effect of heat release time, t_{HR}. There is no simple analytical estimate for t_{HR} so the definition was arbitrarily chosen to be the time required for 95% of the injected mass to be consumed. The most direct way to effect the heat release time is through the droplet size distribution. Case 13 is the same as 4, but D_g has been increased to 10 micrometers. This results in a value $t_{HR}/t_{BD} = 0.55$. The extent of chamber pressure oscillations as represented by P^* is reduced from 3 to 1.7. In Case 14 $D_g = 10$ but σ_g is increased to 2.0 so the distribution is no longer monodisperse. This results in further attenuation of chamber pressure oscillations. The larger, slower burning droplets introduce a time delay in the heat release which dampens chamber pressure oscillations. The magnitude of chamber pressure oscillations can be recovered by reducing t_{BD}/t_{PULSE}.

Rapid heat release is desirable because it allows for a smaller value for t_{BD} which translates into a smaller, lighter combustion chamber. However, if heat release is too rapid then it will not be possible to complete injection during the low-pressure part of the cycle. Figure 7 shows the effect of finite duration injection on the rate of chamber pressure rise. The injection event is broken up into 10 discrete pulses evenly spaced in time. Case 4 is used as the baseline, but droplet size has been increased to 10 microns to be representative of the class of injectors

contemplated for this type of device. Chamber pressures histories are shown for injection durations of 0, 1, 2 and 3 milliseconds. As the time required for injection increases the final pressure at the end of injection increases.

Satellite Applications

Previous studies of the potential benefits for pulsed combustors, including pulse detonation rocket engines, have focused on improvements in specific impulse, however, for space applications, the improvements in theoretical performance are minimal because large expansion ratios can be achieved with low chamber pressures produced by pressure-fed feed systems. Space payoffs for pulsed rockets will ultimately be determined by comparing an optimized pulsed rocket system with an optimized conventional system, however, in order to determine if there is enough potential to warrant further investment, basic sensitivity studies such as the following must first be performed.

We consider a typical application for chemical propulsion on a satellite: a pressure-fed, 450 Newton, apogee engine. We consider two scenarios for replacing the existing thruster with a pulsed thruster. In the first scenario the spacecraft manufacturer wishes to increase the Isp of the thruster, but cannot accept an increase in the nozzle exit area due to space envelope restrictions. The manufacturer wishes to retain the existing propellant systems as much as possible, including propellants, operating pressures and flowrates. In the second scenario, the manufacturer would like to reduce feed pressures to reduce feed system component weights without sacrificing performance.

	Constant Pressure Baseline	Pulsed Engine Scenario 1	Pulsed Engine Scenario 2
Thrust (N)	450	450	450
Min. Pc (MPa)	0.69	0.69	0.26
Max. Pc (MPa)	0.69	3.00	1.10
Flow (Kg/s)	0.143	0.141	0.143
Area Ratio	164	375	164
Throat Dia. (cm)	1.91	1.26	1.91
Exit Dia. (cm)	24.5	24.5	24.5
Chamb. Dia. (cm)	5.08	3.30	5.08
Length (cm)	60.5	57.2	60.5
Specific Impulse	316	322	316
Engine Mass (Kg)	4.0	5.3	4.75
Tank Mass (Kg)	22.2	22.2	15.9

Table 4 Notional study of pulse combustor replacements for an apogee engine

Engine performance is calculated using the model described above. Dimensions and weights are obtained using the PRO:AIAA program. Results for the baseline, constant-pressure case and the pulsed engine scenarios are given in the table.

Consistent with the stated requirements, the thrust is the same in each case. The space envelope is nearly the same with the nozzle exit diameter the same for each engine and the overall length reduced by 3 cm for pulsed engine scenario 1.

The goals for scenario 1 are achieved through an increase in the average chamber pressure, allowing the same thrust to be achieved with a smaller throat, which in turn allows a higher expansion ratio nozzle to be used without changing the exit diameter. This produces an Isp improvement of 6 seconds. The minimum chamber pressure was assumed to be determined by the feed system and was set at the same value used for the constant pressure engine. The maximum chamber pressure was determined by a practical upper limit on expansion ratio of approximately 375. Engine mass is increased by 1.3 Kg as a result of the higher peak chamber pressure.

The goals for scenario 2 are achieved by decreasing the pressure of the feed system allowing a reduction in tank mass of 6.3 Kg. The average chamber pressure is the same as the baseline case producing an engine of identical dimensions and performance. The increase in peak pressure results in an increase in engine mass of 0.75 Kg, resulting in an overall decrease in mass of 5.5 Kg.

The significance of these changes must be considered within the context of satellite economics. The useful lifetime of a satellite is generally limited by the propulsion system. A rule of thumb for satellite operations is that a 1 second improvement in Isp corresponds to approximately 50 days of station-keeping and a six second improvement corresponds to an additional year. Also, one month on station in geosynchronous orbit requires approximately 2

Kg of propellant and 5.5 Kg of additional propellant corresponds to approximately three additional months. Each additional month on station is worth several million dollars in revenue. The potential payoff from the two scenarios are in the range of tens of millions of dollars per satellite, fully justifying the cost of developing these systems.

Conclusion

It has been shown that the potential benefits of pulse detonation propulsion can also be realized using a simpler explosion-cycle system. The ignition system and buffer gas injection can be eliminated. Extremely high pressures associated with detonations of condensed phases can be avoided.

The specific impulse of a pulsating rocket is the same as a steady state rocket operating with the same average mass flow and throat area. This sets the value of the equivalent steady state chamber pressure which determines the performance. The nozzle area ratios optimize at the same value.

There are three characteristic times that control explosion-cycle engine operation: injector pulsing period, chamber blowdown time, and heat release time. The heat release time depends on both the intrinsic burning rate of the propellant and the time required for injection. For the cycle to operate the heat release time must be less than the chamber blowdown time, which in turn must be less than the injector pulsing period. The magnitude of chamber pressure oscillation was shown to depend on two non-dimensional time scales, the ratio of chamber blow down time to the injector pulsing period, and the ratio of the heat release time to the chamber blow down time.

Acknowledgements

This work was supported by the Propulsion Directorate of the Air Force Research Laboratory. Many valuable suggestions and discussions with Doug Talley are gratefully acknowledged.

References

1. Talley, D.G., Coy, E.B., "Constant Volume Limit of Pulsed Propulson for a Constant γ Ideal Gas," Journal of Propulsion and Power, Vol. 18, No. 2, 2002, pp. 400-406
2. Bratkovitch, T.E., Aarnio, M.J., Williams, J., Bussing, T.R.A., "An Introduction to Pulse Detonation Rocket Engines," AIAA 97-2742, 33rd AIAA/ASME/SAE/ASEE Joint Propulsion Conference, 1997
3. Zipkin, M.A., Lewis, G.W., "Analytical and Experimental Performance of an Explosion-Cycle Combustion Chamber for a Jet-Propulsion Engine," NACA Tech. Note 1702, 1948
4. Lu, Y.C., Boyer, E., Koch, D., Kuo, K.K., "Measurement of Intrinsic Burning Rate of Nitromethane", AIAA paper 97-3107, 1997
5. Brown, C.D., PRO:AIAA Propulsion Design Software, AIAA, 1995

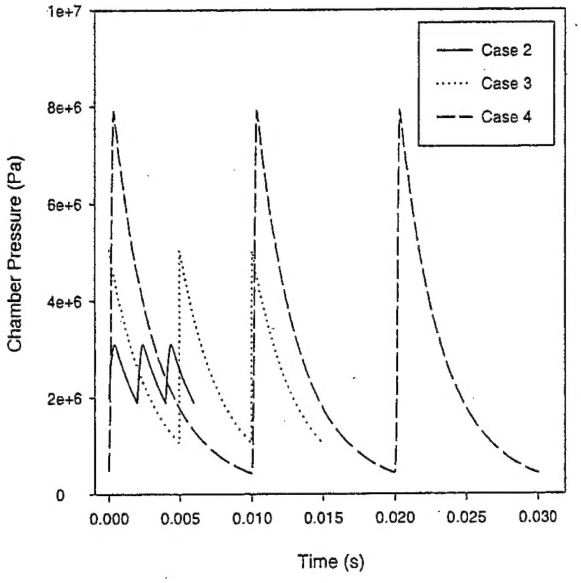

Figure 1. Effect of injection frequency on chamber pressure for a fixed engine geometry. Heat release occurs instantaneously.

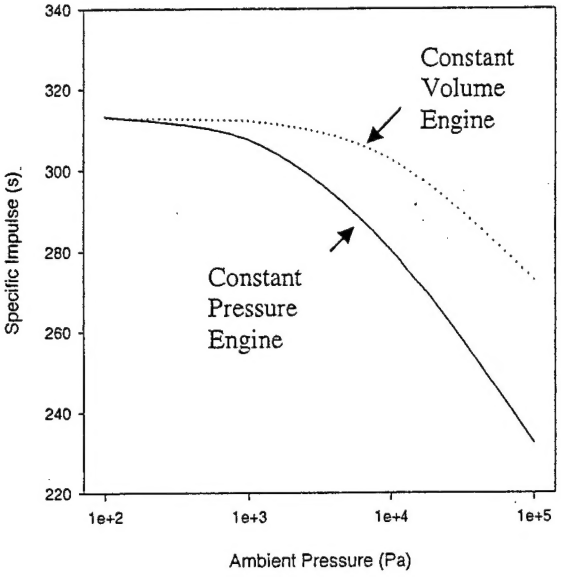

Figure 2. Specific impulse as a function of ambient pressure. Performance advantage of pulsed propulsion increases at high ambient pressure.

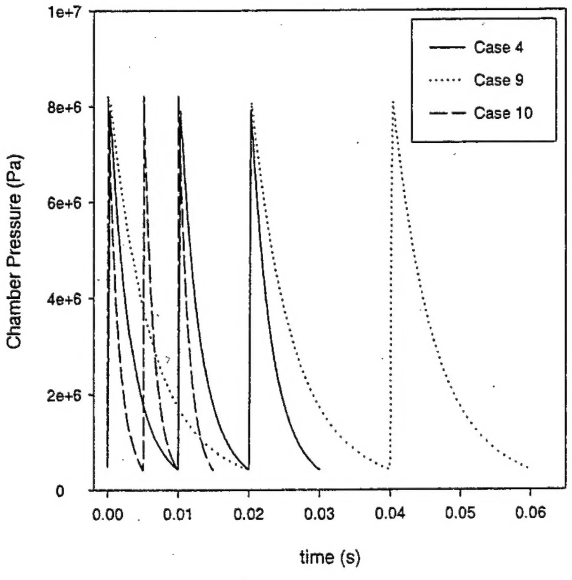

Figure 3. Chamber pressure oscillations for chambers with varying geometry and operating frequency. The magnitude of pressure oscillations is a function of the blowdown time and injector pulsing period only.

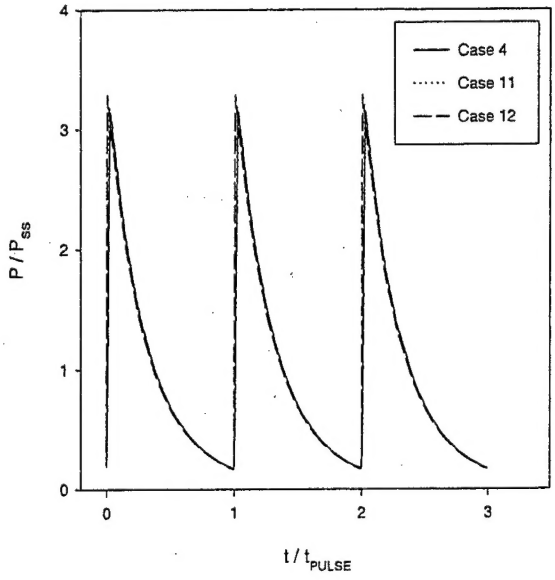

Figure 4. Chamber pressure plotted in non-dimensional coordinates showing that the pressure history is a function of the ratio of blowdown time to injector pulsing period.

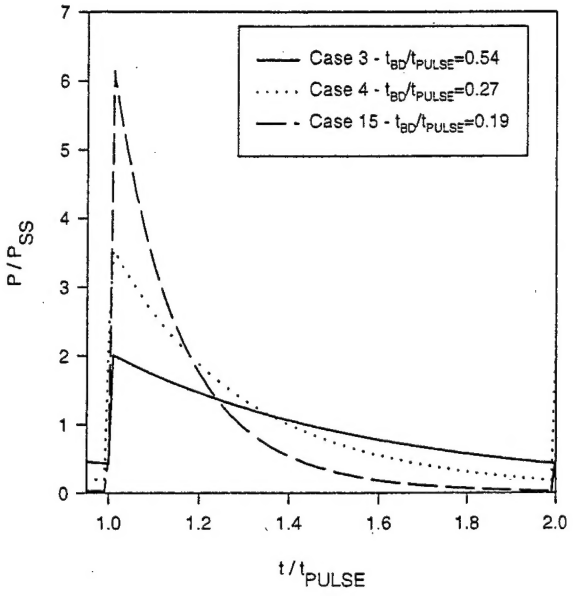

Figure 5. Effect of varying the ratio of blowdown time to injector pulsing period in the limit of short heat release time.

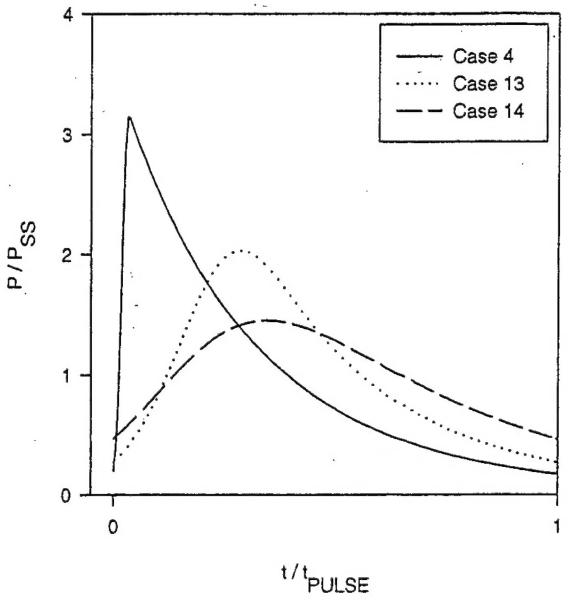

Figure 6. Effect of finite heat release time on chamber pressure oscillations

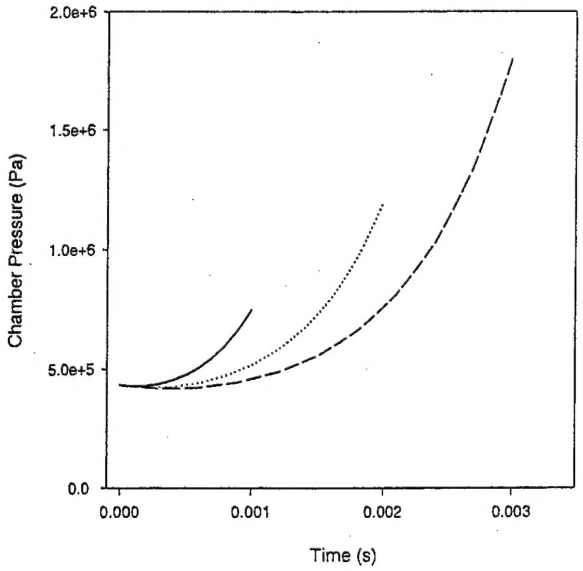

Figure 7. Effect of finite injection duration on rate of chamber pressure rise. Chamber pressure must not exceed injector discharge pressure during the injection.